JOURNAL OF VIROLOGY, June 1979, p. 805-820
0022-538X/79/06-0805/16$02.00/0

Vol. 30, No. 3

Isolation and Localization of Herpes Simplex Virus Type 1 mRNA

KEVIN P. ANDERSON, JAMES R. STRINGER,† LOUIS E. HOLLAND, AND EDWARD K. WAGNER*

Department of Molecular Biology and Biochemistry, University of California at Irvine, Irvine, California 92717

Received for publication 4 December 1978

Herpes simplex virus (HSV) DNA bound to cellulose has been used as a reagent to isolate viral mRNA for size analysis on denaturing agarose gels. Total viral polysomal polyadenylated RNA was isolated from cells late after infection when such RNA has sequences encoded by approximately 45% of the HSV DNA. This RNA has a size range of from 1.5 to ≥8 kilobases, with certain sizes, such as 1.7 to 1.9 kilobases, being favored. We have used the restriction endonucleases *Hin*dIII and *Xba*I singly and together to generate various sized fragments covering the entire HSV-1 genome. These fragments have been bound to cellulose to allow isolation of HSV-1 mRNA annealing to different regions of the viral genome. Discrete sizes of viral mRNA are associated with certain regions of the genome, but the mRNA population hybridizing to even the smallest restriction fragments is complex. We used hybridization of size-fractionated RNA to Southern blots of restriction fragments of HSV-1 DNA generated by the *Bgl*II as well as *Hin*dIII and *Xba*I endonucleases to confirm the preparative hybridization data and to provide some overlap data for positioning transcripts. The data of blot and preparative hybridization agreed very well and were combined to construct a preliminary transcription map of HSV-1. Such a map revealed at least two areas of the long unique region of the HSV-1 genome which annealed to a large number of HSV-1 transcripts. Furthermore, discrete-sized mRNA species larger than 5 kilobases in length were found only in the middle of the long unique region. The implications of these data are discussed.

Herpes simplex virus type 1 (HSV-1) is a large DNA virus which replicates in the nucleus of infected cells. At least 48 HSV-1-specific proteins, at least half of which are structural proteins, have been identified in infected cells by using sodium dodecyl sulfate-polyacrylamide gels (11). The virus particle contains double-stranded DNA having a guanine-plus-cytosine content of 67% (23). The molecular weights of various strains of HSV-1 DNA have been reported to be between 95×10^6 and 100×10^6 (8, 32), corresponding to an approximate length of 140,000 to 150,000 base pairs (140 to 150 kilobase [kb] pairs). The particular strain of HSV-1 DNA used in this study (KOS) is 28.1 times the length of the relaxed replicative form of ϕX174 (34), corresponding to a length of 150 kb pairs based on the known length of this phage DNA (3). HSV DNA is structurally complex and has been shown to consist of a long region and a short region, each composed of unique sequences bounded by different inversely repeated sequences (24). Each of these two regions may be linked to the other by either end, resulting in four equimolar configurations of the viral DNA (9, 39).

Transcription of this genome has been studied in our laboratory and in several others, with general agreement on the following points. In cells infected at moderate multiplicity, HSV DNA synthesis begins about 3 h postinfection (p.i.) and reaches a maximum rate by 6 h p.i. Before the onset of viral DNA synthesis, abundant RNA transcripts from 20 to 25% of the viral genome are found associated with polyribosomes (15, 28, 31). Both "Southern blot" hybridization and RNA displacement loop hybridization of HSV RNA have shown that these early HSV mRNA species map throughout the HSV-1 genome (7, 29). The abundant, early HSV-1 mRNA species can be differentiated into two classes. One class consists of the immediate-early or α mRNA's, which are found in high abundance in the cytoplasm of cells treated with cycloheximide from the time of infection (15). The α mRNA species have been shown, by both blot hybridization and solution hybridization to isolated restriction fragments of HSV-1 DNA, to be transcribed from defined, noncontiguous re-

† Present address: Cold Spring Harbor Laboratory, Cold Spring Harbor, NY 11724.

gions of DNA comprising 10 to 12% of the viral genome (7, 14). The other major abundant class of mRNA species found prior to viral DNA replication is the β messages. These mRNA's encode proteins which are synthesized only after proteins encoded by the α mRNA species have been synthesized (12).

At times after infection when viral DNA synthesis is maximal (late), the majority of early RNA sequences continues to be synthesized (7, 33), and transcripts from an additional 15 to 20% of the viral genome are also found on polyribosomes in good yield. These are the γ, or late, mRNA species. At least a portion of these γ mRNA species has been detected even at the earliest times after infection, but at a concentration 10- to 20-fold lower than the α and β mRNA classes (15, 28, 30). At this time after infection (late), as much as 90% of newly synthesized polyadenylated [poly(A)] RNA on polyribosomes in the infected cell is viral (28). Furthermore, it has been extensively shown that all the sequences in viral mRNA can be isolated as poly(A) RNA (25, 28).

mRNA molecules of HSV-1 associated with the polyribosomes of infected cells resemble mRNA molecules of other DNA viruses and eucaryotic cells. HSV-1 mRNA, in addition to being polyadenylated, is capped at the 5′ end (4, 20), and we have found its average size to be no less than 2 kb (28). However, due in part to the large size and complexity of the HSV genome, little has been reported concerning the properties and origins of individual viral mRNA species.

In this study, we have used two independent methods to determine the size ranges of specific HSV-1 mRNA species synthesized late after infection and to localize individual transcripts to specific regions of the viral genome. We have used restriction fragments of HSV-1 DNA bound to cellulose to purify viral mRNA homologous to these restriction fragments. Size fractionation on denaturing agarose gels of viral mRNA obtained in this manner reveals a characteristic pattern of specific-size mRNA species homologous to each restriction fragment. In addition to such characteristic species, all regions of the viral genome hybridize to a complex pattern of minor species of viral mRNA. The size distributions of viral mRNA encoded by different regions of the HSV-1 genome also have been determined by first fractionating infected-cell mRNA on denaturing agarose gels and then hybridizing size fractions to Southern blots of HSV-1 restriction fragments. The major species and less prominent discrete species of viral mRNA seen in RNA preparatively hybridized to restriction fragments are readily identifiable by using this procedure. The results of both types of experiments have been used to construct a preliminary transcription map of the HSV-1 genome. This map shows the minimum number of discrete mRNA species consistent with our data.

MATERIALS AND METHODS

Cells and virus. Monolayer cultures of HeLa cells were grown at 37°C in Eagle minimal essential medium containing 10% calf serum and no antibiotics. Plaque-purified virus of the KOS strain of HSV-1 was used for all infections.

Preparation of RNA. Monolayer cell cultures (2×10^7 cells per T-150 flask) were infected for 30 min with 10 PFU of virus per cell and overlaid with modified medium 199 containing Earle salts (Flow Laboratories) supplemented with 5% fetal calf serum. For ^{3}H-labeled RNA, the cells were labeled from 5.25 to 6 h p.i. with 15 μCi of [^{3}H]uridine (28 Ci/mmol; Schwarz/Mann) per ml in medium 199 containing 5% dialyzed fetal calf serum. For ^{32}P-labeled RNA, the cells were labeled from 2 to 6 h p.i. with 200 μCi of carrier-free [^{32}P]orthophosphate (New England Nuclear) per ml in Eagle minimal essential medium containing 1/10 the normal phosphate concentration and 5% dialyzed fetal calf serum.

Polyribosome-associated RNA was isolated by the magnesium precipitation method of Palmiter (22) as described by Stringer et al. (28). After phenol extraction and ethanol precipitation, poly(A) RNA was purified from the total polyribosome-associated RNA, using oligodeoxythymidylic acid-cellulose (Collaborative Research). Poly(A) RNA was bound to the cellulose in 0.5 M NaCl–0.1 M Tris (pH 7.6)–1 mM EDTA, rinsed thoroughly, and eluted in a solution containing 0.01 M Tris (pH 7.6) and 1 mM EDTA. This procedure results in 50% of the ^{3}H radioactivity and 15% of the ^{32}P radioactivity in polyribosome-associated RNA being recovered as poly(A) RNA. A single T-150 flask typically yielded 4 to 5 μg of poly(A) RNA with specific activities of 120,000 and 200,000 cpm/μg, respectively, when ^{3}H labeled and ^{32}P labeled. Radioactivity was measured as a 1% solution in Aquasol II scintillation fluid (New England Nuclear) in a Beckman LS-230 scintillation counter.

This poly(A) RNA has been shown to be intact by the following criteria. Recovery of 5′ cap structure from poly(A) RNA isolated in this manner is virtually quantitative (20), demonstrating no appreciable breakage between the 3′ poly(A) tail and the 5′ cap. Furthermore, this poly(A) RNA serves as an extremely efficient template for in vitro translation, and the polypeptide products migrate in sodium dodecyl sulfate-polyacrylamide gels as sharp bands corresponding to proteins synthesized in vivo, with little or no background of partial translation products as would be seen with nicked or degraded template RNA (Anderson et al., unpublished data).

Preparation of HSV DNA. Cells grown in plastic roller bottles (10^8 cells per bottle) were infected with 10 PFU of virus per cell and incubated in medium 199 containing 5% fetal calf serum. For ^{32}P-labeled DNA, the cells were overlaid at 4 h p.i. with phosphate-free Eagle minimal essential medium containing 5% dialyzed fetal calf serum and 25 to 50 μCi of [^{32}P]ortho-

phosphate per ml. The cells were scraped into the medium after 24 h, collected by low-speed centrifugation (2,000 × *g* for 5 min), and resuspended in 0.01 M NaCl–0.01 M Tris (pH 7.4)–3 mM $MgCl_2$–0.5% Nonidet P-40. The cells were lysed by 6 to 10 strokes in a tight-fitting Dounce homogenizer, and nuclei were removed by low-speed centrifugation. Virus was pelleted from the cytoplasmic supernatant by centrifugation at 27,000 × *g* for 20 min. The virus pellet was solubilized in 0.1 M NaCl–0.02 M EDTA–0.01 M HEPES (*N*-2-hydroxyethyl piperazine-*N'*-2-ethanesulfonic acid) (pH 7.8)–1% Sarkosyl and digested with proteinase K (250 μg/ml) for 3 h at 55°C. The DNA was banded by CsCl-isopycnic centrifugation as previously described by Wagner et al. (35), and DNA at 1.725 g/ml (>90% of DNA in gradient) was collected and dialyzed against an appropriate restriction endonuclease buffer. A total of 25 to 50 μg of purified HSV DNA is recovered from 10^8 cells by this procedure.

Restriction endonuclease digestion of HSV-1 DNA and fractionation of resulting fragments. Restriction endonucleases *Hin*dIII, *Xba*I, and *Bgl*II were purchased from New England Biolabs. All digestions were performed under conditions recommended by the supplier. Enzyme, at 1 U/4 μg of DNA, was incubated with DNA for 2 h at 37°C. Double digestion with *Hin*dIII and *Xba*I enzymes was performed by digesting first with *Hin*dIII and then adjusting the salt concentration and adding β-mercaptoethanol before digesting with *Xba*I enzyme.

Restricted DNA (30 to 100 μg) was fractionated by electrophoresis in two 7.5-cm tracks in 0.5% agarose, horizontal slab gels (42 by 20 by 1.2 cm) for 48 h at 60 V (80 mA). Electrophoresis buffer was 0.04 M Tris (pH 7.8)–0.005 M sodium acetate–2 mM EDTA–0.5% ethidium bromide. Bands were visualized by using long-wave UV light.

DNA was isolated from excised bands by dissolving the agarose in 5 M $NaClO_4$ at 60°C and absorbing DNA to hydroxyapatite as described by Wilkie and Cortini (39). After elution in 0.5 M sodium phosphate (pH 6.8), the DNA was extracted with isopentylalcohol to remove any remaining ethidium bromide, desalted on a Sephadex G-50 column, and ethanol precipitated.

Binding of DNA to diazotized cellulose. Total HSV DNA, as well as restriction fragment DNA, was bound to diazotized cellulose by a modification of the procedure of Noyes and Stark (21). *m*-Aminobenzyloxymethyl cellulose (Miles Laboratories) was reprecipitated and diazotized as described in reference 21. However, for rinses and coupling, 10 mM potassium phosphate (pH 6.5) was used as a buffer instead of 0.2 M sodium borate (pH 8.0). DNA, in 80% dimethyl sulfoxide and 2 mM potassium phosphate at concentrations of 100 to 200 μg/ml for total HSV DNA and 25 to 50 μg/ml for restriction fragment DNA, was heated to 78°C for 5 min, cooled to 4°C, and then mixed with the diazotized cellulose so that the cellulose concentration was 10 mg (dry weight)/ml. When less than 10 μg of DNA was being manipulated, *Escherichia coli* DNA was added as carrier to bring the concentration to 10 μg. The cellulose suspension was mixed continuously at 4°C for 48 h and then rinsed twice with 80% dimethyl sulfoxide and 2 mM potassium phosphate at 50°C, four times with 0.1× SSC (0.15 M NaCl plus 0.015 M sodium citrate) at 25°C, three times with 98% formamide and 0.01 M HEPES (pH 8.0), and three times with hybridization buffer (80% formamide, 0.4 M Na^+, 0.1 M HEPES [pH 8.0], 0.005 M EDTA). ^{32}P-labeled DNA was included in each reaction so that the efficiency of coupling could be monitored. A total of 35 to 45% of input radioactivity remained bound to the cellulose after rinsing. DNAcellulose contained 5 to 10 μg of DNA per mg of cellulose for total DNA and 1 to 3 μg/mg of cellulose for restriction fragment DNA. DNA coupled to cellulose was stored in hybridization buffer under nitrogen at 4°C.

Hybridization of RNA to cellulose-bound DNA. ^3H-labeled, poly(A) RNA was hybridized to cellulose-bound DNA for 4 h at 57°C in hybridization buffer containing recrystallized formamide. For total HSV DNA bound to cellulose, 1 to 2 μg of RNA (1×10^5 to 2×10^5 cpm) was hybridized with 5 to 10 μg of cellulose-bound DNA. For restriction fragments bound to cellulose, 10 to 20 μg of RNA was hybridized to 15 μg-equivalents of DNA bound to cellulose (1 μg-equivalent is the amount of restriction fragment corresponding to digestion of 1 μg of intact HSV DNA). The hybridization mixture was agitated every hour to avoid settling of the cellulose. After hybridization, the cellulose was rinsed four times with 2× SSC at 25°C, twice with hybridization buffer at room temperature, and five times with hybridization buffer at 60°C. Hybridized RNA was eluted in 98% formamide and 10 mM HEPES (pH 8.0) at 60°C. The eluant was diluted to a final formamide concentration of 22% and adjusted to 0.1 M sodium acetate, and the eluted RNA was ethanol precipitated.

Methylmercury agarose gels. RNA was fractionated by electrophoresis on 1.4% agarose gels (15 by 0.6 cm) containing 10 mM methylmercury hydroxide (Alpha) as described by Bailey and Davidson (2). Gels were run for 4 to 6 h at 3 mA/gel (2.5 V/cm). After electrophoresis, the gels were soaked in 50 mM β-mercaptoethanol for 20 min and sliced at 2- or 3-mm intervals. The ^3H radioactivity in each slice was measured by dissolving slices in 0.3 ml of 7% perchloric acid at 72°C and mixing with 4 ml of Aquasol. ^{32}P radioactivity of each slice was determined by Cerenkov radiation counting of intact slices.

Preparation and hybridization of DNA Southern blots. Slab gels of restriction endonuclease digests were blotted onto nitrocellulose paper (BA 85, Schleicher & Schuell) in 10× SSC, using the method of Southern (27). The DNA-containing blots were cut into 4-mm strips for hybridization to the RNA contained in individual slices of methylmercury agarose gels. Agarose gels containing 10 to 15 μg of ^{32}P-labeled poly(A) RNA were soaked in 15 mM β-mercaptoethanol for 30 min and cut into 2- or 3-mm slices. Slices containing ^{32}P-labeled RNA were dissolved by heating to 72°C in a solution containing 0.4 M Na^+, 0.1 M HEPES (pH 7.8)–0.005 M EDTA, and 65% formamide. The dissolved ^{32}P-labeled RNA then was hybridized for 24 to 36 h at 57°C in sealed plastic bags containing individual nitrocellulose strips. Strips then were rinsed for three 2-h periods at 48°C in hybridization buffer and 65% formamide, arranged in their original order from the blot, wrapped in Saran wrap, and pressed next to Kodak X-omat-R X-ray film for 24 to 72 h.

RESULTS

Size range of HSV-1 mRNA. Polyribosomal poly(A) RNA, labeled in HSV-1-infected HeLa cells with a 45-min [^{3}H]uridine pulse at 5.25 h after infection, was hybridized to HSV-1 DNA bound to cellulose as described in Materials and Methods. The hybridized RNA (15 to 20% of the input radioactivity) was eluted from the cellulose and subjected to electrophoresis on denaturing agarose gels containing methylmercury hydroxide. Such gels exhibit a linear relationship between the log size of RNA and the distance migrated (2). The size, in kb, of HSV-1 mRNA species was determined by comparing the distance migrated by HSV-1 mRNA species to the distance migrated by ^{32}P-labeled HeLa rRNA species, which were added to the sample as internal size markers. Figure 1 shows that distinct size species of HSV-1 mRNA ranging from >8 to ~1 kb are readily distinguishable. There is a rather large proportion of viral RNA in the size range of 1.9 to 1.7 kb, a dearth of viral mRNA that is 2.1 to 2.7 kb in size, and quite a significant amount of viral mRNA larger than 5 kb. In a large number of preparative hybridizations, the size range and discrete species of viral RNA detected were invariant, but there was some variability in the amount of radioactivity recovered in the size ranges shown. The amount of viral RNA between 10 and 2.5 kb varies between 55 and 65% of the total viral RNA recovered. Such variation is not correlated with the specific preparation of DNA cellulose used in a given experiment.

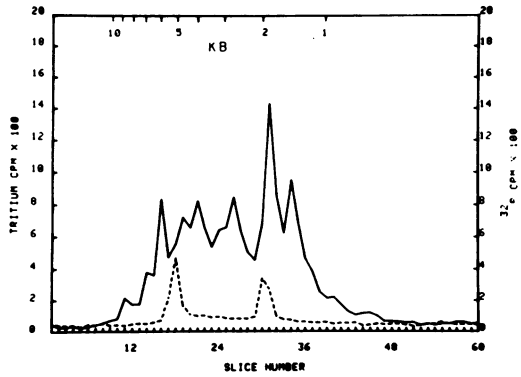

FIG. 1. *Size distribution of HSV-1 mRNA. ^{3}H-labeled polysomal poly(A) mRNA from cells late after infection was hybridized to 15 μg of HSV-1 DNA bound to cellulose, and the HSV-specific mRNA eluted (see text). This viral mRNA was mixed with ^{32}P-labeled HeLa cell rRNA and fractionated by electrophoresis on a 0.6- by 15-cm gel made of 1.4% agarose containing 10 mM methylmercury hydroxide (2). Electrophoresis was for 4 h at 3 mA (2.5 V/cm). The gel was fractionated in 2-mm slices, and the radioactivity was determined. The size of 18S rRNA was taken to be 0.67 ± 0.07 × 10^6 daltons (2,000 bases, 2 kb) and that of 28S rRNA, 1.76 ± 0.15 × 10^6 daltons (5.2 kb) (17, 37). Size extrapolations were based on the fact that RNA migration is a logarithmic function of RNA size as shown by Bailey and Davidson (2) and discussed in Holm et al. (10).*

To establish that the viral RNA purified by hybridization to cellulose-bound HSV-1 DNA is an accurate representation of the actual population of HSV-1 RNA labeled during the pulse period, we tested our hybridization procedure for specificity and for its ability to leave RNA undegraded. Two experiments established the specificity of cellulose-bound HSV-1 DNA for viral sequences. When [^{3}H]uridine-labeled, uninfected HeLa cell poly(A) polyribosomal RNA was incubated with cellulose-bound HSV-1 DNA, only 0.05 to 0.10% of the radioactive HeLa RNA was bound to the cellulose after our standard rinsing procedure. Equivalent amounts of poly(A) polyribosomal RNA from infected cells yielded from 15 to 20% hybrids. Analysis of nonspecifically bound uninfected cell RNA on methylmercury agarose gels showed no significant peaks of radioactivity migrating in any given size range.

In a second experiment to test the specificity of hybridization to cellulose-bound DNA, poly(A) polyribosomal RNA from infected cells was hybridized to cellulose-bound *E. coli* DNA. Again, less than 0.1% of input amounts of material bound to the cellulose. That which did bind showed no peaks of radioactivity on methylmercury gels.

Two control experiments demonstrated that there is no appreciable degradation of HSV-1 mRNA during the hybridization and elution procedure. First, ^{32}P-labeled HeLa cell rRNA was incubated under hybridization conditions and then run on denaturing gel electrophoresis. No evidence of degradation of RNA could be seen by either an alteration in the ratio of the 28S rRNA to 18S rRNA or the appearance of increased RNA migrating heterogeneously. In the second control experiment, ^{3}H-labeled poly(A) polyribosomal RNA was isolated from infected cells and directly sized on a methylmercury agarose gel. The gel was sliced, and each slice was assayed for viral RNA by hybridization to HSV-1 DNA in a manner similar to that described by Weiss et al. (36). Detailed results of this experiment will be presented elsewhere (Holland et al., submitted for publication). It suffices here to report that the distribution of HSV-specific RNA detected by hybridization across the gel was essentially identical to that of HSV RNA

isolated by hybridization to cellulose-bound HSV-1 DNA.

We conclude from these control experiments that preparative hybridization of viral mRNA with HSV DNA bound to cellulose under our conditions gives an accurate and reproducible representation of the population of viral mRNA species present in the isolated RNA population. As has been discussed in Materials and Methods, our evidence that the RNA is not degraded during our isolation is excellent; therefore, we conclude that the DNA-cellulose hybridization gives us a valid representation of viral RNA labeled during the pulse period. This is confirmed by our findings (Anderson et al., unpublished data) that DNA-cellulose-hybridized RNA is an efficient template for in vitro translation, and the protein products show no indication of mRNA degradation.

Identification of HSV-1 mRNA species encoded by different regions of the viral genome. The *Hin*dIII, *Xba*I, *Bgl*II, and *Hin*dIII/*Xba*I double-digest restriction endonuclease sites in the prototypical arrangement of the DNA of our strain (KOS) of HSV-1 are shown in Fig. 2. These enzymes cleave the viral DNA molecule into a number of fragments which migrate as individual bands on agarose gels. Gel bands were shown to contain single DNA fragments by blotting the gels onto nitrocellulose (27) and hybridizing with ^{32}P-labeled overlapping fragments from different restriction endonuclease digests. Sites generated by the other three arrangements of the viral DNA are described in the legend to Fig. 2.

The restriction fragments of HSV-1 DNA, shown in Table 1, were isolated from agarose gels and bound to cellulose (Materials and Methods). Individual cellulose-bound HSV-1 DNA restriction fragments then were used to isolate viral RNA molecules containing sequences homologous to that DNA fragment. We have used 15 μg-equivalents of restriction fragment bound to cellulose as a standard amount of DNA in our hybridizations. We define the amount of any given restriction fragment derived from 1 μg of total HSV-1 DNA as 1 μg-equivalent of that fragment. In this manner, the concentrations of DNA sequences in the cellulose-bound restriction fragments were kept in the same proportion as would occur in a hybridization using 15 μg of total HSV-1 DNA bound to cellulose.

Three controls accompanied each hybridization to cellulose-bound HSV-1 DNA restriction

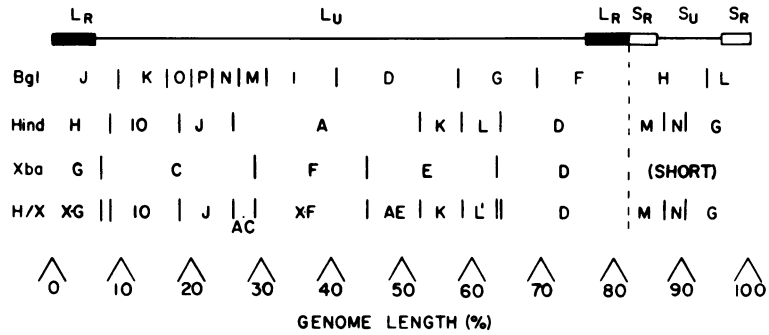

FIG. 2. *Map of restriction endonuclease fragments of the KOS strain of HSV-1. These maps are based on published maps for these sites (18, 26, 38). We have confirmed them for our strain (KOS) of HSV-1 as described previously (29). The fragments generated by cleavage by the restriction endonucleases BglII, HindIII, XbaI, and HindIII/XbaI double digests are shown for the prototypical arrangement (P) of our HSV-1 strain. The solid boxes at the ends of the long segment represent the long repeat (L_R) sequences; the open boxes on the short segment represent the short repeat (S_R) sequences. Three other arrangements occur (9, 39). These are I_L, where the long segment is inverted relative to the short; I_S, where the short segment is inverted relative to the long; and I_{LS}, where both the long and short segments are inverted relative to the prototype. These arrangements have no effect on the yield of fragments which are totally contained by cleavage sites in either the long or short segment, but do lead to submolar bands for fragments coming from the ends of molecules and those bridging the junction between the long and short segments. Submolar fragments for the endonucleases shown are as follows. Half-molar fragments arise from ends of molecules: BglII L and HindIII G are from P and I_L. BglII J, HindIII H, XbaI A (XbaI D + short region), and XbaI G are from P and I_S. BglII F, HindIII D, XbaI B (XbaI G + short region), and XbaI D are from I_L and I_{LS}. BglII H and HindIII M are from I_S and I_{LS}. Quarter-molar fragments arise as the sum of the half-molar fragments from either side of the junction for each arrangement: BglII A is F + H, and HindIII C is D + M. These regions are contiguous in P. BglII B is J + H, and HindIII F is H + M. These regions are contiguous in I_L. BglII C is F + L, and HindIII B is D + G. These regions are contiguous in I_S. BglII E is J + L, and HindIII E is H + G. These regions are contiguous in I_{LS}. XbaI has no cleavage sites in the short segment; therefore, the half-molar fragments XbaI A and XbaI B have both arrangements of the short region.*

TABLE 1. *HSV-1 endonuclease fragments isolated for DNA-cellulose binding*

Fragment[a] (source)	Mol wt (×10⁶)	Size[b] (kb pairs)	Molarity[c]	Region of genome represented[d]
(X)G	6.9	10.5	0.5[e]	Long repeat
(H)IO	9.5	14.4	1	
(H)J	7.5	11.4	1	
(H/X)AC	3	4.5	1	
(X)F	15.5	23.5	1	Long unique
(H/X)AE	7.3	11.1	1	
(H)K	6	9.1	1	
(H)L	5.4	8.2	1	
(H)C	22.2	33.6	0.25[e]	Long unique Long repeat Short repeat
(H)M	4.7	7.1	0.5[e]	Short repeat
(H)N	3.1	4.7	1	Short unique
(H)G	8.9	13.5	0.5[e]	Short unique Short repeat
H(F)	12.8	19.4	0.25[e]	Long repeat Short repeat

[a] (X) is derived from an *Xba*I digest; (H) is from an *Hin*dIII digest; (H/X) is from a *Hin*dIII/*Xba*I double digest.

[b] Based on 1 kb pair having a molecular weight of 6.6×10^5.

[c] Based on the fourfold arrangement of the HSV-1 genome as described in the legend to Fig. 2.

[d] See Fig. 2.

[e] Submolar fragments are derived from the four possible arrangements of the HSV-1 genome described in the legend to Fig. 2. Thus, X(G) is from P and I_S, H(C) is from P, H(M) is from I_S and I_{LS}, H(G) is from P and I_L, and H(F) is from I_L.

fragments. (i) A small amount of the RNA sample to be hybridized was fractionated in parallel with the preparatively hybridized RNA on denaturing agarose gels; (ii) a sample of the RNA to be hybridized to cellulose-bound restriction fragment DNA was hybridized to total HSV-1 DNA bound to cellulose and the hybrids were fractionated in parallel with the hybrids to the restriction fragment; (iii) ^{32}P-labeled HeLa rRNA was added to the hybridization mixture, and radioactivity which did not bind to the cellulose also was fractionated in parallel with the hybridized RNA at the end of the hybridization period. The quality of each sample of RNA obtained by each preparative hybridization was evaluated on the basis of the control experiments. The RNA was deemed intact and representative if no degradation of the unhybridized RNA and ^{32}P-labeled rRNA was apparent and if the RNA purified by hybridization to total cellulose-bound HSV-1 DNA looked typical (see Fig. 1). All DNA fragments show hybridization efficiencies roughly comparable to fragment size (Table 2).

The size distributions of RNA purified by hybridization to different HSV-1 restriction fragments are shown in Fig. 3. The panels are arranged to represent regions of the HSV-1 genome starting with the left end of the L region through the S region of the P arrangement. From this figure, it is evident that certain viral mRNA species are associated with certain restriction fragments. However, in all cases, the mRNA population homologous to a given restriction fragment is complex. Some RNA species migrate as major sharp bands, suggesting very defined sizes for these mRNA species, which are synthesized in high, or at least moderate, abundance. RNA migrating sharply at a size of 6 kb hybridizes to *Hin*dIII fragment J and *Hin*dIII/*Xba*I double-digest fragment AC (Fig. 3C and D). A discrete 9.6-kb species is found in RNA hybridized to *Hin*dIII/*Xba*I double-digest fragment AE (Fig. 3F). *Hin*dIII fragment K hybridizes efficiently with three discrete RNA species, 7.2, 5.2, and 3.8 kb in size (Fig. 3G). Sharply migrating RNA species 3 and 1.9 kb in size hybridize to *Hin*dIII fragment L (Fig. 3H). Other RNA bands migrate broadly, suggesting a heterogeneity of sizes. A relatively large amount of such material is seen in RNA that hybridizes to *Xba*I fragment F (Fig. 3E). The RNA species that hybridizes to *Hin*dIII fragment G (Fig. 3K) also is illustrative of such size heterogeneity. Note in particular the broadness of the peak centered at 1.9 kb, which covers a range of sizes from 1.6 to 2.2 kb. Other discrete and heterogeneous size classes of RNA homologous to HSV-1 restriction fragments are indicated in Table 2.

Certain trends can be discerned from examination of Fig. 3 and Table 2. For example, RNA ranging in size from 1.6 to 2 kb is a major component of RNA hybridizing to total HSV DNA and hybridizes to all of the restriction fragments shown. Such RNA is a major component of the RNA hybridizing to all but three of these restriction fragments (*Hin*dIII fragments J and K and *Hin*dIII/*Xba*I double-digest fragment AE). Conversely, only one fragment (*Hin*dIII fragment IO) has sequences homologous to a well-resolved RNA species (2.6 kb) between 2.1 and 2.7 kb. Discrete peaks of RNA >5.5 kb are found to hybridize to only four fragments (*Hin*dIII fragments J and K and *Hin*dIII/*Xba*I double-digest fragments AE and AC). It is clear, however, that heterodisperse RNA, up to about 8 kb in size, can be detected in RNA hybridizing to most fragments.

Some of the restriction fragments examined have common DNA sequences. This is a consequence of the rearrangement of the long and short segments generating the four isomeric configurations of the genome and the presence of

TABLE 2. *HSV mRNA species hybridizing to restriction fragment DNA-cellulose*

Restriction fragment[a]	Hybridization efficiency (%)[b]	Size (kb) of:[c]		Proportion of radioactivity migrating >5 kb
		Prominent mRNA species	Resolvable mRNA species	
(X)G[d]	1.3	2.8 1.9	4.3 1.4	0.16 (B)[e]
(H)IO	1.4	4.4 ± 0.4 2.6 1.9		0.15
(H)J	1.6	6 4.8 ± 0.3 4.2 ± 0.2	3.0 ± 0.2 2 1.8 1.5	0.24
(H/X)AC	0.6	6 2.9 1.9 ± 0.15	5.2 4.5 3.9	0.24
(X)F	3.9	4.2 ± 0.2 3.3 ± 0.2 1.9 1.3	8.4[f]	0.32 (B)
(H/X)AE	1.2	4.1 2.8 ± 0.3 1.6 ± 0.25	9.6 6.5 5.2	0.19
(H)K	1.1	7.2 5.2 3.8	2.9 1.9	0.32
(H)L	0.83	2.8 1.9	5.2 4.4 1.6	0.12
(H)C[d]	1.35	1.9	4.8 4.1 2.8	0.14
(H)N	0.8	1.9 1.5	4.5 ± 0.4 2.7 ± 0.2 1.0	0.2 (B)
(H)G[d]	1.2	3.1 ± 0.2 1.9 ± 0.3	4.2 ± 0.2	0.13 (B)
(H)M[d]	0.36	1.9	4.4 2.8 ± 0.2	0.10
(H)F[d]	1.1	2.0	4.3 2.8 1.6	0.09

[a] See Fig. 2.

[b] In all cases, 1×10^6 to 2×10^6 cpm of ^{3}H-labeled polysomal poly(A) RNA was used. Hybridization was carried out with 15 μg-equivalents of the fragment DNA bound to cellulose and RNA fractionated as described in Fig. 3.

[c] Size of RNA species is based on the position of 28S and 18S rRNA markers (see Fig. 1). When a region of migrating RNA was broad enough to indicate size heterogeneity, the range of size values is indicated.

[d] Fragments (X)G, (H)C, (H)G, (H)M, and (H)F are generated by only certain arrangements of the HSV-1 genome as described in the legend to Fig. 2 and in Table 1.

[e] (B) indicates that the RNA species >5 kb in size migrate as a polydisperse range.

[f] This band is only partially resolved.

the inverted repeat sequences. For example, the entire sequence of *Hin*dIII fragment M is contained within *Hin*dIII fragments C and F, and the short repeat sequence which comprises better than 90% of *Hin*dIII fragment M also is contained in *Hin*dIII fragment G. All three of these fragments exhibit homologous RNA of the same sizes found for *Hin*dIII fragment M. The sizes of RNA hybridizing to *Xba*I fragment G and *Hin*dIII fragments C and F are similarly consistent with the sequences shared by these fragments.

Localization of specific viral transcripts on the HSV-1 genome. As an independent check for the DNA-cellulose fractionation of HSV mRNA, as well as to provide some limited overlap data for mapping HSV mRNA species, we carried out a number of DNA hybridizations

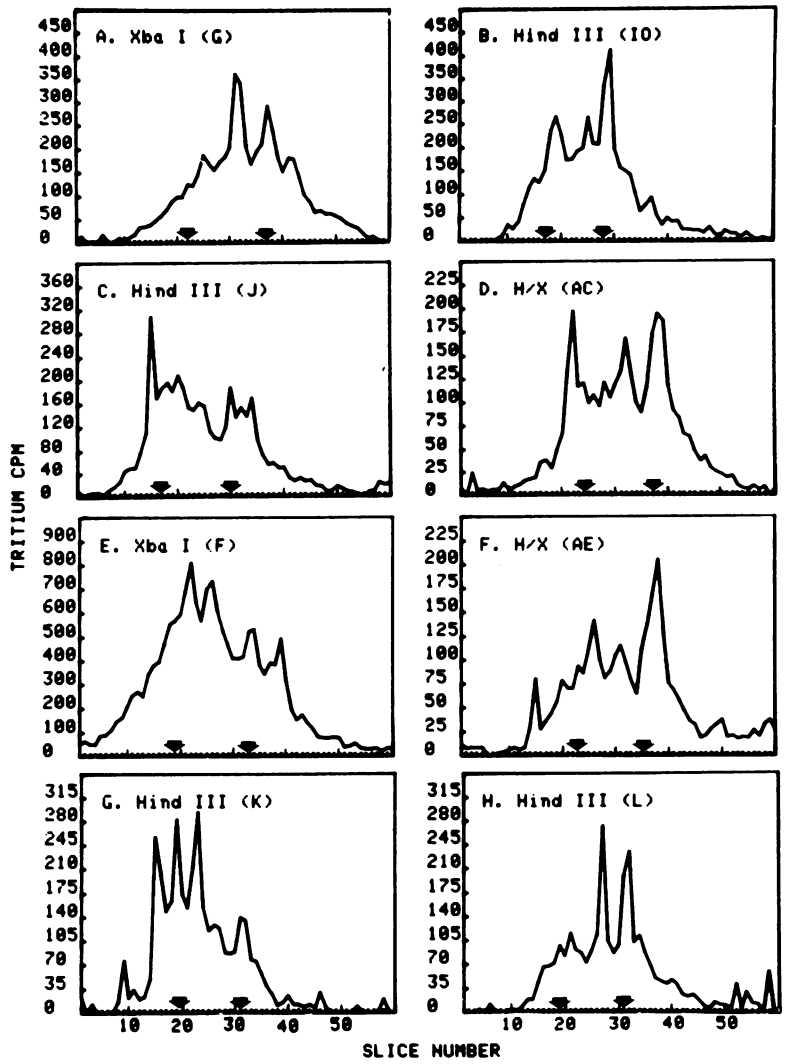

FIG. 3. *Size distribution of HSV-1 mRNA hybridized to restriction fragments of viral DNA. (A) through (M) are denaturing agarose gels of viral RNA hybridized to HSV-1 restriction fragments from different regions of the genome (see Table 1). The fragments are arranged so as to represent regions beginning from the left of the L region through the short region of the P arrangement. In each panel, polysomal poly(A) RNA from 4 × 10^7 to 8 × 10^7 cells was hybridized to 15 μg-equivalents of restriction fragment DNA cellulose. Specific amounts of DNA cellulose used and hybridization efficiencies are shown in Table 2. Details of RNA labeling and gel fractionation are as described in the legend to Fig. 1 and in the text. The arrows on each panel show the position of the ^{32}P-labeled HeLa rRNA included as an internal-size marker.*

of size-fractionated RNA to Southern blots of restricted DNA. Polysomal poly(A) mRNA was labeled for 4 h with ^{32}P, isolated from infected cells, and fractionated on methylmercury agarose gels. The longer labeling time was necessary to get RNA of sufficient specific activity for blot hybridization. Gels were sliced into 2- or 3-mm slices, and Cerenkov radiation was determined. Radioactivity profiles obtained were quite reproducible, and a typical one is shown in Fig. 4. Parallel gels with a small amount of the ^{32}P-labeled RNA and ^{3}H-labeled HeLa cell rRNA showed that the two peaks of indicated radioactivity migrated with sizes of 6.0 and 1.9 kb. These two peaks were used as internal size markers in all blotting experiments. The slices were dissolved in hybridization buffer containing 65% formamide (see Materials and Methods), and RNA from individual gel slices was hybridized to nitrocellulose strips containing restriction

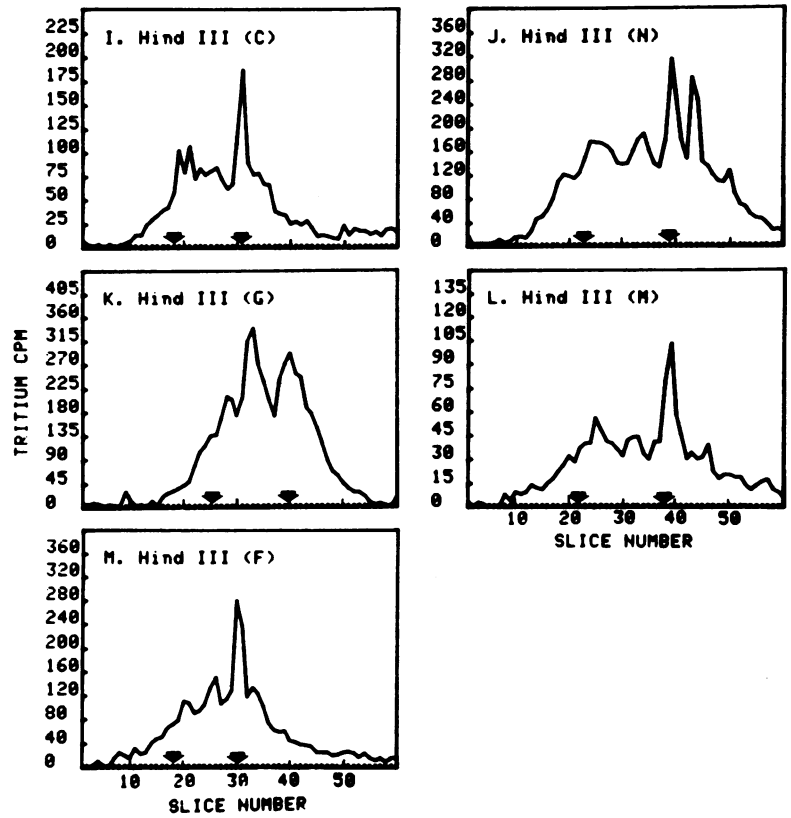

FIG. 3—continued

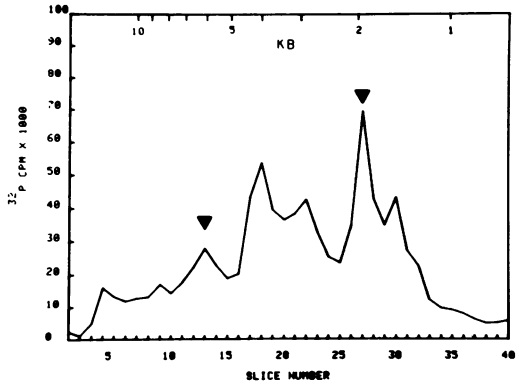

FIG. 4. *Size distribution of polysomal poly(A) RNA from HSV-1-infected HeLa cells. In the experiment shown, [^{32}P]RNA from 8 × 10^7 cells labeled from 2 to 6 h p.i. with [^{32}P]orthophosphate was fractionated on a denaturing agarose gel as described in the legend to Fig. 1. The gel was divided into 2-mm slices, and radioactivity was determined by counting Cerenkov radiation. The size range of the RNA was determined as described in Fig. 1, using 6- and 1.9-kb peaks (arrows) described in the text as size markers. Only the top two-thirds of the profile is shown.*

fragments of HSV-1 DNA. After hybridization, the strips were rinsed, assembled in order of RNA size, and autoradiographed. Representative blot hybridizations to *Hin*dIII/*Xba*I double-digest fragments and *Bgl*II fragments are shown in Fig. 5. Hybridizations to blots of *Hin*dIII fragments also were performed (not shown). Table 3 summarizes the results of our blot hybridization data. We have shown the size and location of the RNA species which hybridized to defined fragments of the HSV-1 genome. The qualitative correlation between preparatively hybridized RNA and blot-hybridized RNA is excellent (cf. Tables 2 and 3). For example, RNA migrating at 6 kb, which hybridized to cellulose-bound *Hin*dIII fragments J and *Hin*dIII/*Xba*I fragment AC (Fig. 3C and D), appears as highly radioactive spots in blots of those same fragments (Fig. 5A) and in the overlapping *Bgl*II fragments N and P (Fig. 5B). The discretely migrating RNA species isolated by hybridization to *Hin*dIII fragment K (Fig. 3G) also appear as discrete spots on blots of this fragment (Fig. 5A). The rare 2.6-kb size mRNA species in *Hin*dIII fragment IO is found in blots to this fragment as

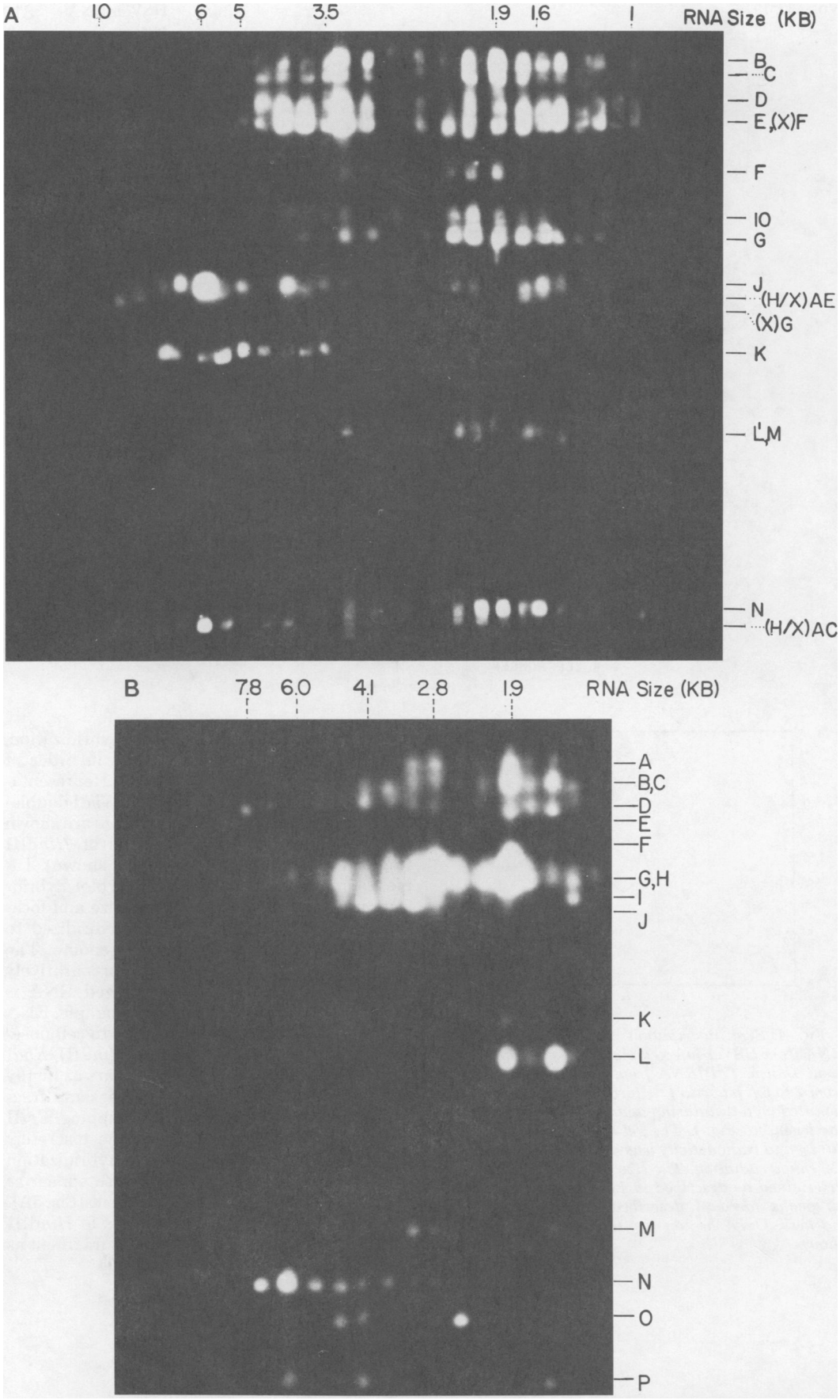
A
10
6
5
3.5
1.9
1.6
1
RNA Size (KB)
B
C
D
E,(X)F
F
10
G
J
(H/X)AE
(X)G
K
L,M
N
(H/X)AC
B
7.8
6.0
4.1
2.8
1.9
RNA Size (KB)
A
B,C
D
E
F
G,H
I
J
K
L
M
N
O
P

well as to *BglII* fragment O, which is contained in it. The congruence between the DNA-cellulose data and the blot hybridization data also holds for the broadly migrating viral RNA species. Examination of the RNA homologous to *Hin*dIII fragment G (Fig. 3K) shows a large and broad peak of radioactivity that is 2.2 to 1.6 kb in size. In the blots, there is extensive hybridization of RNA in this size range to *Hin*dIII fragment G and *BglII* fragment L. In addition to the 6-kb species, the RNA hybridizing to *Hin*dIII fragment J bound to cellulose migrates as a complex mixture of partially resolved sizes that range from 5 to 3 and 2 to 1.5 kb (Fig. 3C). RNA hybridizing to blots of this fragment, as well as to the component *BglII* fragments P and N, show a similar range of sizes. A significant portion of the RNA hybridizing to *Xba*I fragment F DNA-cellulose migrates broadly in the size range of 5 to 3 kb (Fig. 3E); and RNA hybridizing to blots of *BglII* fragments I and D, which overlap *Xba*I fragment F, also migrates broadly in this size range.

Quantitative comparison between the amount of RNA of a particular size hybridizing to a given blot of a restriction fragment and that isolated from the same fragment bound to cellulose is difficult. This is because the RNA for blot hybridization was labeled for 4 h compared to 45 min for the preparative hybridization, and because exact quantitation of the amount of radioactivity hybridizing to a blot is difficult due to differential efficiency of transfer of large and small DNA fragments. However, it is clear that, at a first level of approximation, the two methods give similar results.

There is, however, one notable quantitative difference between the methods. In experiments with blotted DNA, very little RNA hybridizes to the long repeated sequences present in *Xba*I fragment G and *BglII* fragment J. In contrast, RNA pulsed from 5.25 to 6 h p.i. hybridized well to cellulose-bound *Xba*I fragment G. In experiments using labeling times of 0 to 2 h p.i., described elsewhere (Holland et al., submitted), several discrete sizes of RNA hybridized efficiently to blots of *Xba*I fragment G. The result is consistent with there being reduced transcription from these regions late, compared to early, after infection. A second possibility is that RNA transcribed from this region from 2 to 6 h p.i. has a rapid turnover rate, resulting in a lower steady-state concentration of this RNA in the infected-cell compared to other RNA species. This RNA would be represented to a greater extent in short pulse-labeled RNA (used for preparative hybridization) than in long-term labeled RNA (used in blot hybridization). Clements et al. (7) also described a reduced efficiency of hybridization to blots of the long repeat region with RNA labeled from 0 to 7 h p.i.

DISCUSSION

Complexity of HSV-1 mRNA. We have measured the size of HSV-1 RNA species synthesized during a time late in infection when viral DNA synthesis is proceeding at a rapid rate and when 80 to 90% of the single-strand equivalent of the viral genome is expressed as mRNA in at least moderate abundance. There are few significantly labeled species smaller than 1.5 kb and little viral mRNA which migrates as a discrete size species larger than 8 to 9 kb (Fig. 1). Within this range, there are certain favored sizes, such as 6, 5.4, 3, and especially 1.8 to 2.2 and 1.5 to 1.6 kb. Also, one size class, that between 2 and 3 kb, is rare for HSV-1 mRNA. The lack of HSV-1 mRNA 2 to 3 kb in size appears to be peculiar to viral RNA since uninfected HeLa cells do not lack mRNA in this size range (data not shown). HSV proteins have been reported to range in size from 15,000 to at least 250,000 daltons (11). The largest size of HSV-1 mRNA isolated in reasonable yield (8 to 9 kb) could readily encode the largest polypeptides. On the other end of the spectrum, it is interesting that the smallest HSV mRNA species seen in any quantity are no smaller than 1.2 kb, a size with

FIG. 5. *Hybridization of size-fractionated HSV-1 mRNA to DNA restriction fragment blots. Total ^{32}P-labeled polysomal poly(A) RNA from infected cells was fractionated as described in the legend to Fig. 4. Individual slices were dissolved in 0.4 M Na^+, 0.1 M HEPES (pH 7.8), 5 mM EDTA, and 65% formamide (see text) and hybridized to strips of Southern blots of HSV-1 DNA, either double-digested with HindIII and XbaI endonucleases (A) or digested with BglII endonuclease (B). The locations of the cleavage sites for these enzymes on HSV-1 DNA are shown in Fig. 2. After hybridization and rinsing (see text), strips were assembled in order of size of RNA used and radioautographed with Kodak X-omat-R film. Both radioautographs were exposed for 24 h at −70°C with a Kodak intensifying screen, and contact prints of the X-ray film are shown. Size of RNA in the slices was determined from the migration of the 6- and 1.9-kb RNA species as described in the legend to Fig. 4. Positions shown for restriction fragments in the blot were determined by visualization of the fractionated fragments of DNA before blotting. Resolution after blotting was checked by incubating a strip with total ^{32}P-labeled RNA (not shown). In the case of the double-digest blot, the bands are as described in the footnotes to Table 1; all bands are HindIII fragments except when indicated as an Xba fragment (X) or a double-digest fragment (H/X).*

TABLE 3. *Localization of HSV-1 mRNA by blot hybridization*

*Bgl*II restriction fragment[a]	Size of RNA hybridizing[b] (kb)	*Hin*dIII/*Xba*I double-digest restriction fragment[a]	Size of RNA hybridizing[b] (kb)
J	2.8–3(−) 1.9(−)	X(G)	2.8(−) 1.9(−)
K	3.2–4(−) 1.9		
O	4–4.6 2.5(+) 1.9	H(IO)	3–4.6 2.6 2.0(+) 1.6–1.9
P	6 4.1 1.5	H(J)	6.5 6(+) 5.2 4(+) 3.5(−) 1.9–2.1 1.5–1.7(+)
N	6.7 6(+) 2.8–5.2 1.9(−)		
M	4.6(−) 2.8–3.2 1.9 1.5	H/X(AC)	6(+) 4.3 3.2 1.9–2.1
I	9.8(−) 3.2–4.6(+) 1.9 1.2		
D	9.8(−) 7.8 5.2(−) 4.1 2.8–3.6 1.6–1.9	H/X(AE)	8.6 3.8 2.8(−) 1.7
		H(K)	7.1(+) 5.2–5.6(+) 3.5–3.8 1.7–1.9(−)
		H(L)[c]	2.8–3.1(+) 1.9(+) 1.5–1.7
A	4(−) 2.8–3.2 1.9(+) 1.5	H(D)	4–4.8(+) 3–3.5(+) 2.5(−) 1.5–2.1(+)
		H(M)[c]	2.8(−) 1.9–2.1(+) 1.7
L	1.9(+) 1.5(+)	H(N)	3 1.9–2.1(+) 1.6(+)
		H(G)	4(−) 3–3.2 1.5–2.3(+)

[a] Fragments are arranged in relative order on the prototype arrangement (see Fig. 2). Data are shown only for those fragments which are clearly resolved.

[b] Based on the position of 6- and 1.9-kb RNA in gels (see text). Slices yield a size ±7% of the stated values. Very intense spots are indicated with a (+) and faint ones are indicated with a (−).

[c] Based on blots of *Hin*dIII digests which resolve fragments L and M.

at least twice the coding capacity necessary for translation of a 15,000-dalton protein. Whereas about half of the identified viral polypeptides are smaller than 60,000 daltons, most mRNA species are 1.8 to 1.9 kb and greater in size, providing more coding capacity than required. Since little posttranslational processing has been observed (11), this suggests that many HSV-1 molecules can contain significant amounts of untranslated sequences.

The viral mRNA which hybridizes to even the smallest restriction fragments of HSV DNA is a complex mixture of sizes which, in some cases, exceeds the asymmetric coding capacity of the fragment even when only the most prominent species are considered. *Hin*dIII fragment K (9.1 kb pairs in length) hybridizes efficiently with three highly labeled viral mRNA species whose aggregate size is over 16 kb. *Hin*dIII/*Xba*I fragment AC is only 4.5 kb pairs in length, yet hybridizes with mRNA species totaling well over 10 kb. Also, there are at least four species of viral RNA >3.5 kb in size hybridizing to the region encompassed by *Bgl*II fragments P and N, whose total length is approximately 9 kb. One explanation for complex patterns of RNA species binding to a given region is that some species of mRNA hybridizing to specific DNA restriction fragments are encoded by a DNA sequence which bridges a restriction endonuclease site. This appears to be the case for the 6-kb mRNA which hybridizes to both *Hin*dIII fragment J and *Hin*dIII/*Xba*I fragment AC (see below). However, most cases cannot be explained this simply. For example, with *Hin*dIII fragment K, we know from the hybridization patterns of neighboring DNA fragments that at least two of the large RNA molecules which hybridize to *Hin*dIII fragment K do not significantly extend into the sequences adjacent to this small piece of DNA (Table 3). The aggregate size of these two species is 12 kb, which is 3 kb more than could be asymmetrically transcribed from *Hin*dIII fragment K. Again, the localization of the RNA species >3.5 kb hybridizing to *Hin*dIII fragment J and *Bgl*II fragments P and N cannot be explained by RNA overlapping into neighboring fragments. Such an apparent "transcriptional overload" in a given region can be explained by a combination of the following: (i) symmetric transcription, (ii) asymmetric transcription and processing of RNA-producing species which have overlapping nucleotide sequences, (iii) RNA splicing events resulting in the mRNA molecules being homologous to more than one locale on the genome. Symmetric transcription probably does not significantly contribute since <2% of 1-h pulse-labeled poly(A) polyribosomal RNA from infected cells is self-complementary (13; Stringer and Wagner, unpublished data). Since both RNA species containing shared sequences and spliced transcripts have been observed in papova- and adenoviruses (1, 5, 6), it is reasonable to expect herpesviruses to exhibit similar complexity in transcription and processing of viral RNA. Overlapping mRNA sequences would be indicated experimentally if 3′ ends of several specific mRNA sizes could be localized into a small region of the genome contiguous with the restriction fragment containing the bulk of the sequences homologous to the RNA. Preliminary results of such studies suggest overlapping sequences of HSV-1 mRNA do, in fact, occur (Holland et al., submitted).

In addition to the large number of specific-sized mRNA species found in localized regions of the HSV-1 genome, there are also appreciable amounts of heterogeneously migrating RNA found hybridizing to all restriction fragments. This RNA is viral since it is not found in control experiments using uninfected cells or *E. coli* DNA bound to cellulose. There are a number of possible sources of this heterogeneously migrating viral RNA. Certainly, some could arise by degradation of RNA during workup or hybridization. We have already shown that such degradation is quite limited, however. Furthermore, in several cases, similar patterns of such heterogeneously migrating RNA are seen no matter whether the RNA is size fractionated before or after hybridization. Therefore, we feel this precludes degradation being the only source of such heterogeneously migrating RNA. Some RNA species may well be present in small amounts and would not resolve well from more abundant species. Small amounts of specific-sized mRNA species hybridizing to a given restriction fragment could also arise from low-efficiency hybridization of RNA whose sequences barely overlap into the fragment. Another possible source of small amounts of RNA of heterogeneous size would be the presence in the polysomal poly(A) RNA of partially processed viral RNA species derived from a larger precursor. Such species have been found for both adenovirus and simian virus 40 (5, 16). A fifth source of small amounts of specific sizes of RNA could result from transcription of all four arrangements of the HSV genome (see Fig. 2). It has been reported that only one or two of the arrangements of HSV-1 DNA are able to yield viable progeny virus (18); however, other arrangements could be transcribed to produce viral RNA species whose processing could be abortive. The relative contribution of any of these possible sources of the viral RNA species present in low abundance will be resolved by continued analysis of HSV-1 transcription.

Preliminary transcription map of HSV-1. The combined DNA-cellulose and blot hybridization data allow us to localize a number of viral mRNA size species in restriction fragments. We have constructed a preliminary transcription map based on our data as shown in Fig. 6. This map is a simplification of the data summarized in Tables 2 and 3 in that it shows only readily identifiable mRNA species. We have included those mRNA's of discrete sizes which were observed from both DNA-cellulose hybridization and blot hybridization data. Because of the greater resolution of RNA prepared by hybridization to DNA-cellulose, we have used the sizes of Table 2 for individual RNA species. We have indicated single species of RNA which were resolved after DNA-cellulose hybridization even if such could not be resolved by using blot hybridization. When RNA migrated as a range of sizes in both DNA-cellulose and blot experiments, we have shown one species, with brackets indicating the extremes in values.

In most cases, viral transcripts shown in Fig. 6 are aligned in the middle of the restriction fragment containing homologous sequences. In some cases, however, enough information is available to localize mRNA species more precisely. The rationale for localization of the individual RNA species shown is as follows. (i) The low-efficiency hybridization of both *Xba*I fragment G and *Bgl*II fragment J made confirmation of the results of DNA-cellulose hybridization difficult. We have indicated only the two species detected by blot hybridization on the map. It is clear from both the DNA-cellulose hybridization and RNA displacement loop hybridization of early RNA (29) that there is considerable RNA hybridizing to this region in addition to the two species shown. We have rather arbitrarily located these two species to the long repeat, because the unusually low efficiency of RNA blot hybridization suggests an unusual feature of the hybridization. (ii) RNA hybridizing to *Hin*dIII fragment IO cellulose hybridizes mainly to *Bgl*II fragment O, which maps to the right of most of this region. (iii) There are a large number of transcripts hybridizing to the region 20 to 30% of the total genome length in from the left end of the prototype arrangement. The size distributions of RNA hybridizing to *Bgl*II fragments

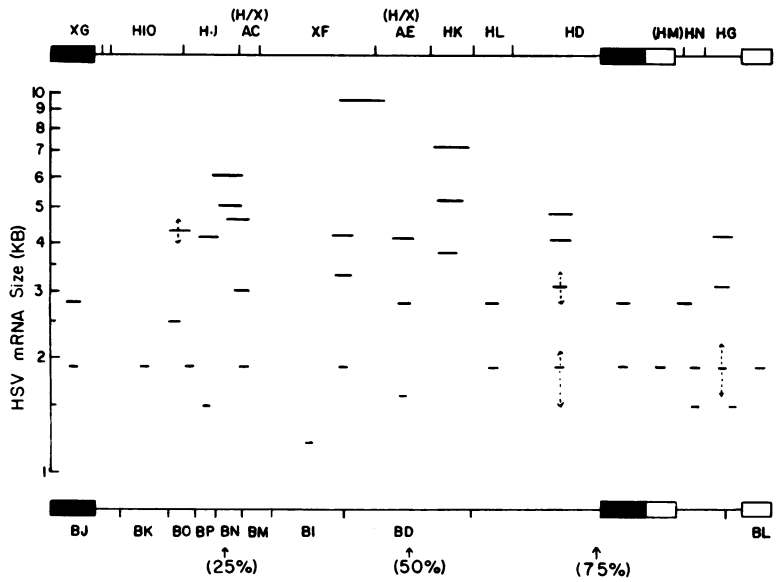

FIG. 6. *Preliminary minimal transcription map of HSV-1 RNA. The data of Tables 2 and 3 and Fig. 3 and 5 have been reduced to a minimal transcription map as described in the text. Only prominently labeled RNA species are included. The location of the XbaI, BglII, and HindIII fragments scored are shown for the P arrangement of HSV-1 DNA. The percent length from the left end of the genome is shown with arrows. When RNA of the same size was found in neighboring restriction fragments, it is shown as a single species bridging the restriction cleavage site, provided the radioactivity in both fragments is equivalent, such as for the 6-kb RNA species in HindIII fragment J and HindIII/XbaI double-digest fragment AC. The length of the lines is proportional to the relative length of the RNA in question. The RNA species with bracketed sizes indicate RNA which migrates broadly in the range shown. The RNA species shown under the region spanned by HindIII fragment D, which arises from the I_L and I_{LS} conformations of the viral DNA, are based on blot data and are shown in the unique region due to the low hybridization of the long repeat region found in XbaI fragment G and BglII fragment J.*

O, P, and N, which subdivide this region, indicate that most of the species of RNA hybridize to the region on either side of the right-hand *Hin*dIII site generating fragment J. (iv) The RNA species of size around 8 to 9 kb found hybridizing to *Xba*I fragment F cellulose corresponds to RNA of this size found in blots of *Bgl*II fragments I and D and *Hin*dIII/*Xba*I double-digest fragment AE. For clarity, we have shown this as a single species, since one RNA molecule of this size is large enough to bridge all the restriction sites generating the fragments. However, preliminary experiments suggest that two discrete 3′ ends for RNA of this size occur in this region (data not shown). We have shown RNA species on either side of the junction between *Xba*I fragment F and *Hin*dIII/*Xba*I double-digest fragment AE, depending on whether RNA of this size also hybridizes to blots of *Bgl*II fragment I. (v) Three RNA species have been shown mapping in *Hin*dIII fragment K because of the resolution of these after preparative hybridization (Fig. 3G). However, the midsized RNA hybridizing to blots of *Hin*dIII fragment K consistently shows a broader size distribution than the 7.4- and 3.8-kb species, suggesting that more than one RNA species may be found in this size range. (vi) The RNA hybridizing efficiently to blots of *Hin*dIII fragment D have been localized to the unique region to the left of the long repeat sequences since RNA hybridizes very poorly to both *Xba*I fragment G and *Bgl*II fragment J, which also contain the long repeat sequence. Finally, (vii) the 4-kb species, as well as a range of smaller species of viral RNA species found hybridizing to *Hin*dIII fragment G cellulose and blots, are shown in the short unique region of this fragment since they do not hybridize to blots of *Hin*dIII fragment M or *Bgl*II fragment L, which, like *Hin*dIII fragment G, contains the short repeat region.

The transcription map shown in Fig. 6 underestimates the number of significantly labeled HSV-1 mRNA species. This is especially true for smaller RNA species found in large restriction fragments such as *Xba*I fragment F. But in spite of this and other limitations, certain patterns in the location of HSV-1 mRNA on the viral genome can be seen. The region of the genome from 10 to 15% in from the left end of the prototype arrangement (*Bgl*II fragment K) hybridizes mainly to RNA of size 1.9 to 2 kb. RNA displacement loop hybridization of early HSV RNA also shows low hybridization in this area (29). At least two regions of the genome, the region 20 to 30% in from the left end (*Hin*dIII fragment J) and the region 50 to 60% in from that end (*Hin*dIII fragments K and L), hybridize to numerous RNA species. Higher-resolution mapping of RNA species in the region covered by *Xba*I fragment F may reveal other such regions. Whereas RNA of 1.6 to 2 kb in size is found throughout the genome, a significant amount of RNA smaller than 1.5 kb (1.2 kb) is found only in *Bgl*II fragment I. Well-resolved RNA larger than 5 kb is found in significant amounts only toward the center of the long unique region of the genome (25 to 60% from the left end); furthermore, little viral mRNA >4 kb in size is found in the short region and in either the long or short repeat sequences of the HSV-1 genome. Specific features of HSV-1 RNA metabolism which result in these patterns are unknown.

Correlation of the transcription map with the HSV-1 genetic map. Of the nearly 50 proteins which have been identified as viral, about half have been localized on the HSV-1 genome by using intertypic recombinants between HSV-1 and HSV-2 (19). It is interesting to note that structural (γ) polypeptides map throughout the long unique region, with a large number mapping between 20 and 30% and another large number between 50 and 60% in from the left end of the genome in the prototype arrangement. The very large structural polypeptide, ICP-2, which would require a large mRNA species to encode it, has been localized in this latter region. These areas of the genome correspond to regions contained by *Hin*dIII fragment J and *Hin*dIII fragments K and L; both regions encode large mRNA species. It should be noted that these two regions are symmetrical around the rotation axis of the long sequence of the HSV-1 genome (see reference 29) so that the question of whether the prototype arrangement or one with the long region inverted is biologically active does not interfere with the correlation. Further correlation of the HSV-1 transcription map with polypeptide maps must await studies on the biological activity of the RNA species we have identified in this report.

ACKNOWLEDGMENTS

We thank B. Gaylord and L. Tribble for excellent technical help. We also thank J. Holland for the gift of HeLa cells.

This work was supported by Public Health Service grant CA 11861 from the National Cancer Institute. K.P.A. was supported by Public Health Service predoctoral training grant GM07311 from the National Institutes of Health.

LITERATURE CITED

1. **Aloni, Y., R. Dhar, O. Laub, M. Horowitz, and G. Khoury.** 1977. Novel mechanism for RNA maturation: the leader sequences of simian virus 40 mRNA are not transcribed adjacent to the coding sequences. Proc. Natl. Acad. Sci. U.S.A. **74**:3686–3690.
2. **Bailey, J. M., and N. Davidson.** 1976. Methylmercury as a reversible denaturing agent for agarose gel electrophoresis. Anal. Biochem. **70**:75–85.
3. **Barrell, B. G., G. M. Air, and C. A. Hutchison III.**

1976. Overlapping genes in bacteriophage φX174. Nature (London) **264**:34–41.
4. **Bartkoski, M., and B. Roizman.** 1976. RNA synthesis in cells infected with herpes simplex virus. XIII. Differences in the methylation patterns of viral RNA during the reproductive cycle. J. Virol. **20**:583–588.
5. **Berget, S., C. Moore, and P. A. Sharp.** 1977. Spliced segments at the 5′ terminus of adenovirus 2 late mRNA. Proc. Natl. Acad. Sci. U.S.A. **74**:3171–3175.
6. **Chow, L. T., R. E. Gelinas, T. R. Broker, and R. J. Roberts.** 1977. An amazing sequence arrangement at the 5′ end of adenovirus 2 messenger RNA. Cell **12**:1–8.
7. **Clements, J. B., R. J. Watson, and N. M. Wilkie.** 1977. Temporal regulation of herpes simplex virus type 1 transcription: location of transcripts on the viral genome. Cell **12**:275–285.
8. **Grafstrom, R. H., J. C. Alwine, W. L. Steinhart, C. W. Hill, and R. W. Hyman.** 1975. The terminal repetition of herpes simplex virus DNA. Virology **67**:144–157.
9. **Hayward, G. S., R. J. Jacob, S. C. Wadsworth, and B. Roizman.** 1975. Anatomy of herpes simplex virus DNA: evidence for four populations of molecules that differ in the relative orientations of their long and short components. Proc. Natl. Acad. Sci. U.S.A. **72**:4243–4247.
10. **Holm, C. S., S. G. Oliver, A. M. Newman, L. E. Holland, C. S. McLaughlin, E. K. Wagner, and R. C. Warner.** 1978. The molecular weight of yeast P1 double-stranded RNA. J. Biol. Chem. **253**:8332–8336.
11. **Honess, R. W., and B. Roizman.** 1973. Proteins specified by herpes simplex virus. XI. Identification and relative molar rates of synthesis of structural and nonstructural herpes virus polypeptides in the infected cell. J. Virol. **12**:1347–1365.
12. **Honess, R. W., and B. Roizman.** 1974. Regulation of herpesvirus macromolecular synthesis. I. Cascade regulation of the synthesis of three groups of viral proteins. J. Virol. **14**:8–19.
13. **Jacquemont, B., and B. Roizman.** 1975. RNA synthesis in cells infected with herpes simplex virus. X. Properties of viral symmetric transcripts and of double-stranded RNA prepared from them. J. Virol. **15**:707–713.
14. **Jones, P. C., G. S. Hayward, and B. Roizman.** 1977. Anatomy of herpes simplex virus DNA. VII. α RNA is homologous to noncontiguous sites in both the L and S components of viral DNA. J. Virol. **21**:268–276.
15. **Kozak, M., and B. Roizman.** 1974. Regulation of herpesvirus macromolecular synthesis: nuclear retention of nontranslated viral RNA sequences. Proc. Natl. Acad. Sci. U.S.A. **71**:4322–4326.
16. **Lai, C-J., R. Dhar, and G. Khoury.** 1978. Mapping the spliced and unspliced late lytic SV40 RNAs. Cell **14**: 971–982.
17. **McMaster, G. K., and G. C. Carmichael.** 1977. Analysis of single and double stranded nucleic acids on polyacrylamide and agarose gels by using glyoxal and acridine orange. Proc. Natl. Acad. Sci. U.S.A. **74**:4835–4838.
18. **Morse, L. S., T. G. Buchman, B. Roizman, and P. A. Schaffer.** 1977. Anatomy of herpes simplex virus DNA. IX. Apparent exclusion of some parental DNA arrangements in the generation of intertypic (HSV-1 × HSV-2) recombinants. J. Virol. **24**:231–248.
19. **Morse, L. S., L. Pereira, B. Roizman, and P. A. Schaffer.** 1978. Anatomy of herpes simplex virus (HSV) DNA. X. Mapping of viral genes by analysis of polypeptides and functions specified by HSV-1 × HSV-2 recombinants. J. Virol. **26**:389–410.
20. **Moss, B., A. Gershowitz, J. R. Stringer, L. E. Holland, and E. K. Wagner.** 1977. 5′-Terminal and internal methylated nucleosides in herpes simplex virus type 1 mRNA. J. Virol. **23**:234–239.
21. **Noyes, B. E., and G. R. Stark.** 1975. Nucleic acid hybridization using DNA covalently coupled to cellulose. Cell **5**:301–310.
22. **Palmiter, R. D.** 1974. Mg^{++} precipitation of ribonucleoprotein complexes. Expedient techniques for the isolation of undegraded polysomes and messenger ribonucleic acid. Biochemistry **13**:3606–3614.
23. **Plummer, G., C. R. Goodheart, D. Henson, and C. P. Bowling.** 1969. A comparative study of the DNA density and behavior in tissue cultures of fourteen different herpesviruses. Virology **39**:134–137.
24. **Sheldrick, P., and N. Berthelot.** 1974. Inverted repetitions in the chromosome of herpes simplex virus. Cold Spring Harbor Symp. Quant. Biol. **39**:667–678.
25. **Silverstein, S., R. Millette, P. Jones, and B. Roizman.** 1976. RNA synthesis in cells infected with herpes simplex virus. XII. Sequence complexity and properties of RNA differing in extent of adenylation. J. Virol. **18**: 977–991.
26. **Skare, J., and W. C. Summers.** 1977. Structure and function of herpesvirus genomes. II. Eco RI, Xba I, and Hind III endonuclease cleavage sites on herpes simplex virus type 1 DNA. Virology **76**:581–595.
27. **Southern, E.** 1975. Detection of specific sequences among DNA fragments separated by gel electrophoresis. J. Mol. Biol. **98**:503–517.
28. **Stringer, J., L. Holland, R. Swanstrom, K. Pivo, and E. Wagner.** 1977. Quantitation of herpes simplex virus type 1 RNA in infected HeLa cells. J. Virol. **21**:889–901.
29. **Stringer, J. R., L. E. Holland, and E. K. Wagner.** 1978. Mapping early transcripts of herpes simplex virus type 1 by electron microscopy. J. Virol. **27**:56–73.
30. **Swanstrom, R., K. Pivo, and E. Wagner.** 1975. Restricted transcription of the herpes simplex virus genome occurring early after infection and in the presence of metabolic inhibitors. Virology **66**:140–150.
31. **Swanstrom, R., and E. Wagner.** 1974. Regulation of synthesis of herpes simplex type 1 virus mRNA during productive infection. Virology **60**:522–533.
32. **Wadsworth, S., R. J. Jacob, and B. Roizman.** 1975. Anatomy of herpes simplex virus DNA. II. Size, composition, and arrangement of inverted terminal repetitions. J. Virol. **15**:1487–1497.
33. **Wagner, E., R. Swanstrom, and M. Stafford.** 1972. Transcription of the herpes simplex virus genome in human cells. J. Virol. **10**:675–682.
34. **Wagner, E. K., R. I. Swanstrom, M. Rice, L. Howell, and J. Lane.** 1976. Variation in the molecular size of the DNA from closely related strains of type 1 herpes simplex virus. Biochim. Biophys. Acta **435**:192–205.
35. **Wagner, E. K., K. K. Tewari, R. Kolodner, and R. C. Warner.** 1974. The molecular size of the herpes simplex virus type 1 genome. Virology **57**:436–447.
36. **Weiss, S. R., H. E. Varmus, and J. M. Bishop.** 1977. The size and genetic composition of virus-specific RNAs in the cytoplasm of cells producing avian sarcoma-leukosis viruses. Cell **12**:983–992.
37. **Wellauer, P. K., and I. B. Dawid.** 1973. Secondary structure maps of RNA: processing of HeLa ribosomal RNA. Proc. Natl. Acad. Sci. U.S.A. **70**:2827–2831.
38. **Wilkie, N. M.** 1976. Physical maps for herpes simplex virus type 1 DNA for restriction endonucleases *Hind* III, *Hpa*-1, and *X. bad.* J. Virol. **20**:222–233.
39. **Wilkie, N. M., and R. Cortini.** 1976. Sequence arrangement in herpes simplex virus type 1 DNA: identification of terminal fragments in restriction endonuclease digests and evidence for inversions in redundant and unique sequences. J. Virol. **20**:211–221.